

## Article

# Highly Efficient Biosynthesis of $\gamma$ -Bisabolene with a New Sesquiterpene Synthase AcTPS5 by Dual Cytoplasmic-Peroxisomal Engineering in *Saccharomyces cerevisiae*

Jiajia Liu, Ge Yao, Xiukun Wan , Fuli Wang, Penggang Han, Shaoheng Bao, Kang Wang, Tianyu Song and Hui Jiang \*

State Key Laboratory of NBC Protection for Civilian, Beijing 102205, China; jiajiali0802@163.com (J.L.); bzayaoge@163.com (G.Y.); xiukunwan@126.com (X.W.); wangfuli5728@163.com (F.W.); hanpeng1021@163.com (P.H.); jingwang\_surgeon@yeah.net (S.B.); yiyongjun1949@163.com (K.W.); songtianyu90@foxmail.com (T.S.)

\* Correspondence: ylpkmc@163.com

**Abstract:**  $\gamma$ -bisabolene is a monocyclic sesquiterpene with various biological activities; it has also been approved as a food additive. Additionally, the hydrogenated form of bisabolene is considered as a potential alternative to D2 diesel. *Saccharomyces cerevisiae* has the ability to produce a large amount of acetyl-CoA in both cytosol and peroxisomes, which serves as a precursor in terpene biosynthesis. In this study, AcTPS5 was identified as a new  $\gamma$ -bisabolene synthase. By expressing AcTPS5 and the mevalonate pathway in peroxisomes,  $\gamma$ -bisabolene titer was achieved at 125.0 mg/L. Deleting the peroxisome autophagy gene *atg36* further improved  $\gamma$ -bisabolene production to 216.9 mg/L. The implementation of dual cytoplasmic–peroxisomal engineering further boosted  $\gamma$ -bisabolene production to 296.4 mg/L. Finally, through increasing the acetyl-CoA supply and down-regulating the expression of *ERG9*,  $\gamma$ -bisabolene production was achieved at 584.14 mg/L in shake-flask fermentation and 2.69 g/L in fed-batch fermentation, which is the highest reported production of  $\gamma$ -bisabolene to date. The strategy presented in this study provides an efficient approach for terpene production in *S. cerevisiae*.

**Keywords:**  $\gamma$ -bisabolene; peroxisome; metabolic engineering; *Saccharomyces cerevisiae*



**Citation:** Liu, J.; Yao, G.; Wan, X.; Wang, F.; Han, P.; Bao, S.; Wang, K.; Song, T.; Jiang, H. Highly Efficient Biosynthesis of  $\gamma$ -Bisabolene with a New Sesquiterpene Synthase AcTPS5 by Dual Cytoplasmic-Peroxisomal Engineering in *Saccharomyces cerevisiae*. *Fermentation* **2023**, *9*, 779. <https://doi.org/10.3390/fermentation9090779>

Academic Editor: Debarati Paul

Received: 10 July 2023

Revised: 16 August 2023

Accepted: 18 August 2023

Published: 22 August 2023



**Copyright:** © 2023 by the authors. Licensee MDPI, Basel, Switzerland. This article is an open access article distributed under the terms and conditions of the Creative Commons Attribution (CC BY) license (<https://creativecommons.org/licenses/by/4.0/>).

## 1. Introduction

Sesquiterpenoids are a large family of terpenoid natural products with diverse applications in pharmaceuticals, cosmetics, fragrances, and biofuels; they are typically derived from plants, animals, or microbes [1,2]. Bisabolene is a kind of monocyclic sesquiterpene that is mainly found in plants and fungi. There are three constitutional isomers of bisabolene, i.e.,  $\alpha$ -bisabolene,  $\beta$ -bisabolene, and  $\gamma$ -bisabolene [3]. Hydrogenated products of bisabolene, which have excellent fuel properties, are considered to be potential alternatives to D2 diesel [4]. In addition, each of these isomers has different properties and applications.  $\alpha$ -bisabolene is the main constituent of the oil of chamomile (*Matricaria recutita*), which is used as a herbal medicine [5]. Only a few studies have reported on the biological activity of  $\beta$ -bisabolene, which has been found to exhibit cytotoxicity in breast cancer cell lines and synergistic bactericidal activity against *Staphylococcus aureus* [6,7]. In comparison,  $\gamma$ -bisabolene exhibits various biological activities, such as antibacterial, larvicidal and oviposition deterrent potential, anti-inflammatory, and anti-cancer properties [8–10]. Additionally,  $\gamma$ -bisabolene has been approved as a food additive by the Food and Drug Administration of the United States [11].

Bisabolene is generated from farnesyl diphosphate (FPP) through the catalysis of different bisabolene synthetases in vivo. Since the first  $\alpha$ -bisabolene synthase was identified from *Abies grandis* in 1998, at least 21 sesquiterpene synthases generating different isomers of

bisabolene have been identified, most of which were derived from plants. Three synthases, NvIDS1, PcSTS-08, and BbS, were cloned from insect *Nezara viridula*, fungus *Phanerochaete chrysosporium*, and *Cryptosporangium arvom* bacterium, respectively (Table S1). Due to the challenges in chemical synthesis or plant extraction [12], there is growing interest in the biosynthesis of bisabolene. In 2010,  $\alpha$ -bisabolene synthase (Ag1) from *Abies grandis* was used for  $\alpha$ -bisabolene overproduction through enzyme screening. Through metabolic engineering of *E. coli* and *S. cerevisiae*, a titer of over 900 mg/L  $\alpha$ -bisabolene was achieved in shake-flask fermentation [4]. *Rhodospiridium toruloides* has also been engineered to convert cellulose into  $\alpha$ -bisabolene, with a titer of 318 mg/L [13]. In addition,  $\beta$ -bisabolene and  $\gamma$ -bisabolene were produced through heterologous expression of the  $\beta$ -bisabolene synthase from *Zingiber officinale* and the  $\gamma$ -bisabolene synthase from *Helianthus annuus*, yielding titers of 68.2 mg/L and 20.2 mg/L, respectively [14]. However, these are much lower than the detected levels of  $\alpha$ -bisabolene.

Metabolic engineering is an effective method for developing microbial cell factories to produce high-value compounds. One approach is to engineer metabolic pathways inside subcellular organelles, which can provide a microenvironment for higher productivities [15]. The peroxisomes involved in the  $\beta$ -oxidation of fatty acid are pools of acetyl-CoA in yeast, which have garnered significant interest as a hub for introducing metabolic pathways. For example,  $\alpha$ -humulene was overproduced by introducing  $\alpha$ -humulene synthase into peroxisomes, along with the modification to the cytoplasmic GAL system [16]. Additionally, geraniol and squalene were synthesized in the peroxisomes using a peroxisome acetyl-CoA pool [17,18]. Although there are challenges associated with engineering pathways in peroxisomes, such as insufficient of precursors and negative effects on protein localization, peroxisomes hold great promise for metabolic engineering [19].

In this study, an efficient  $\gamma$ -bisabolene synthase, AcTPS5, was identified and applied for the production of  $\gamma$ -bisabolene in *S. cerevisiae*. Through the introduced FPP pathway enzymes and AcTPS5 in peroxisomes, a titer of 125.0 mg/L  $\gamma$ -bisabolene was achieved. Dual cytoplasmic–peroxisomal engineering of the biosynthesis pathway was applied to further improve  $\gamma$ -bisabolene production. Finally, by increasing the precursor supply and inhibiting the compete pathway, the production of  $\gamma$ -bisabolene reached 2.69 g/L in fed-batch fermentation. This work highlights the potential of dual cytoplasmic–peroxisomal engineering in *S. cerevisiae* for the production of valuable compounds.

## 2. Materials and Methods

### 2.1. Bioinformatic Analysis of Bisabolene Synthases

First, we searched for and downloaded protein sequences of bisabolene synthases from different species, as shown in Table S1. The amino acid sequences of the bisabolene synthases were aligned by ClustalW, and the conserved motifs were analyzed using ES-Prpt 3. The MEGA 11 program based on Jones-Taylor-Thornton was used to generate a bootstrapped maximum-likelihood phylogenetic tree.

### 2.2. Medium, Culture Conditions, and Chemicals

YPD medium (per liter, 10.0 g yeast extract, 20.0 g tryptone, 2% glucose) was used for yeast strain growth. For yeast shake-flask fermentation, YPDG medium (per liter, 10.0 g yeast extract, 20.0 g tryptone, 1% glucose, 1% galactose) was used. SC medium (0.67% yeast nitrogen base, proper amino acid drop-out mix, 2% glucose) was used for yeast strain selection. DNA polymerase and restriction endonucleases were purchased from Vazyme (Nanjing, China) and Thermo Fisher Scientific (Waltham, MA, USA). T4 ligase and Gibson assembly enzyme were purchased from New England Bio-Labs (Ipswich, MA, USA). The primers were ordered from GENEWIZ (Tianjin, China).  $\gamma$ -bisabolene (#B399815, CAS: 13062-00-5) from Toronto Research Chemicals (Toronto, ON, Canada) was used as a standard.

### 2.3. Construction of Plasmids and Strains

The strains and plasmids are listed in Table S2. The primers are listed in Table S3. Plasmids were assembled by overlap PCR, Gibson assembly, and golden gate cloning. The plasmid backbone was derived from pRS462, pEASY-blunt, and pCAS. The corresponding plasmids were transformed into *S. cerevisiae* by the PEG/LiCl method, and gene editing with CRISPR/Cas9 system was mediated by a recyclable gRNA plasmid, as shown in a previous report [20].

pLJJ39 was constructed for expressing the M1 module. For the construction of pLJJ39, the LB of *ROX1*, terminator of *CYC1*, *Actps5*, promoter of *GAL10* and *GAL1*, *ERG20*, terminator of *GAL10* and promoter of *GAL7*, *tHMG1*, terminator of *ADH1*, and RB of *ROX1* were amplified with the primers pPent1-5-F/R, pLJJ39-1-F/R, pLJJ39-2-F/R, pLJJ39-3-F/R, pLJJ39-4-F/R, pLJJ39-5-F/R, pLJJ39-6-F/R, pLJJ39-7-F/R, pLJJ39-8-F/R, and pPent1-4-F/pPent1-8-R, respectively.

pLJJ42 was constructed to express the M2 module. For the construction of pLJJ42, the LB of *EXG1*, terminator of *CYC1*, *Actps5*, promoter of *GAL10* and *GAL1*, *tHMG1*, terminator of *PGK1*, and RB of *EXG1* were amplified with the primers pPent2-2-F/R, pLJJ39-1-F/R, pLJJ42-1-F/R, pLJJ39-3-F/R, pLJJ42-2-F/R, pLJJ42-3-F/R, and pPent2-4-F/R, respectively.

pLJJ148 was constructed to express the M3 module. For the construction of pLJJ148, the LB of *DPP1*, terminator of *CYC1*, *Actps5*, promoter of *GAL10* and *GAL1*, *tHMG1*, terminator of *PGK1*, and RB of *DPP1* were amplified with the primers pLJJ148-1-F/R, pLJJ39-1-F/R, pLJJ42-1-F/R, pLJJ39-3-F/R, pLJJ42-2-F/R, pLJJ42-3-F/R, and pLJJ148-2-F/R, respectively.

pLJJ150 and pLJJ151 was constructed to express the M4 module. For the construction of pLJJ150, the LB of *TRP1*, terminator of *CYC1*, *Actps5*, promoter of *GAL10* and *GAL1*, *tHMG1*, terminator of *PGK1*, and RB of *TRP1* were amplified with the primers pLJJ150-1-F/R, pLJJ39-1-F/R, pLJJ42-1-F/R, pLJJ39-3-F/R, pLJJ42-2-F/R, pLJJ42-3-F/R, and pLJJ150-2-F/R, respectively. For the construction of the plasmid pLJJ151, the sgRNA of *trp1* were amplified with the primers pLJJ151-1-F/R using sgRNA as a template. The truncated *URA3* was amplified from plasmid *KIURA3* with primers pLJJ151-2-F/R. The above fragments were cloned into the *BsaI* site of pCAS.

pLJJ105 was constructed to express the M5 module. For the construction of pLJJ105, the LB of *GAL1*, terminator of *ADH1*, *ERG10-ePTS1*, promoter of *GAL10* and *GAL1*, *ERG13-ePTS1*, terminator of *CYC1*, and RB of *GAL1* were amplified with the primers pLJJ105-1-F/R, pLJJ39-7-F/pLJJ105-2-R, pLJJ105-3-F/R, pLJJ39-5-F/R, pLJJ105-4-F/R, pLJJ105-5-F/pLJJ39-1-R, and pLJJ105-6-F/R, respectively.

pLJJ106 was constructed to express the M6 module. For the construction of pLJJ106, the LB of *911b*, terminator of *ADH1*, *ERG8-ePTS1*, promoter of *GAL10* and *GAL1*, *ERG12-ePTS1*, terminator of *CYC1*, and RB of *911b* were amplified with the primers pLJJ106-1-F/R, pLJJ39-7-F/pLJJ105-2-R, pLJJ106-2-F/R, pLJJ39-5-F/R, pLJJ106-3-F/R, pLJJ105-5-F/pLJJ39-1-R, and pLJJ106-4-F/R, respectively.

pLJJ107 was constructed to express the M7 module. For the construction of pLJJ107, the LB of *LPP1*, terminator of *ADH1*, *tHMG1-ePTS1*, promoter of *GAL10* and *GAL1*, *IDI1-ePTS1*, terminator of *CYC1*, and RB of *LPP1* were amplified with the primers pLJJ107-1-F/R, pLJJ39-7-F/pLJJ105-2-R, pLJJ107-2-F/R, pLJJ39-5-F/R, pLJJ107-3-F/R, pLJJ105-5-F/pLJJ39-1-R, and pLJJ107-4-F/R, respectively.

pLJJ115 was constructed to express the M8 module. For the construction of pLJJ115, the LB of *LEU2*, terminator of *ADH1*, *MVD1-ePTS1*, promoter of *GAL10* and *GAL1*, *ERG20-ePTS1*, terminator of *CYC1*, and RB of *LEU2* were amplified with the primers pLJJ115-1-F/R, pLJJ39-7-F/pLJJ105-2-R, pLJJ115-2-F/R, pLJJ39-5-F/R, pLJJ115-3-F/R, pLJJ105-5-F/pLJJ39-1-R, and pLJJ115-4-F/R, respectively.

For the construction of pLJJ108, sgRNA of *911b*, sgRNA of *GAL1*, truncated *URA3* and pSNR52, sgRNA of *LPP1*, and sgRNA of *LEU2* were amplified with the primers pLJJ108-1-F/R, pLJJ108-1-F/R, pLJJ108-2-F/R, pLJJ108-3-F/R, pLJJ108-4-F/R, and pLJJ108-5-F/R, respectively.

pLJJ147 was constructed to express the M9 module. For the construction of pLJJ147, the LB of *URA3*, promoter of *GAL10*, *Actps5-ePTS1*, terminator of *PGK1*, and RB of *URA3* were amplified with the primers pLJJ147-1-F/R, pLJJ39-3-F/R, pLJJ147-2-F/R, pLJJ147-3-F/R, and pLJJ147-4-F/R, respectively.

For the construction of pLJJ149, the sgRNA of *URA3* was amplified with the primers pLJJ149-1-F/R using sgRNA as a template. The truncated *URA3* was amplified from plasmid KIURA3 with primers pLJJ151-2-F/R. The above fragments were cloned into the *BsaI* site of pCAS.

pLJJ161b was constructed to express the M10 module. The LB of 308a, promoter of *GAL1*, *Actps5-ePTS1* and terminator of *PGK1*, and RB of 308a were amplified with the primers pLJJ161-1-F/R, pLJJ147-2-F/pLJJ147-4-R, and pLJJ161-3-F/R respectively.

pLJJ161 was constructed to express the M11 module. For the construction of pLJJ161, the LB of 308a, terminator of *CYC1*, *tHMG1-ePTS1*, promoter of *GAL10* and *GAL1*, *Actps5-ePTS1*, terminator of *PGK1*, and RB of 308a were amplified with the primers pLJJ161-1-F/R, pLJJ161-2-F/R, pLJJ161-3-F/R, pLJJ39-3-F/R, pLJJ161-4-F/R, pLJJ161-5-F/R, and pLJJ161-6-F/R, respectively.

For the construction of pLJJ163, the sgRNA of 308a were amplified with the primers pLJJ163-1-F/pLJJ149-1-R using sgRNA as a template. The truncated *URA3* was amplified from plasmid KIURA3 with primers pLJJ151-2-F/R. The above fragments were cloned into the *BsaI* site of pCAS.

pLJJ162b was constructed to express the M12 module. The LB of *ypl062w*, promoter of *GAL1*, *Actps5-ePTS1*, terminator of *PGK1*, and RB of *ypl062w* were amplified with the primers pLJJ162-1-F/R, pLJJ147-2-F/pLJJ147-4-R, and pLJJ162-2-F/R respectively.

pLJJ162 was constructed to express the M13 module. For the construction of pLJJ162, the LB of *ypl062w*, terminator of *CYC1*, *tHMG1-ePTS1*, promoter of *GAL10* and *GAL1*, *Actps5-ePTS1*, terminator of *PGK1*, and RB of *ypl062w* were amplified with the primers pLJJ162-1-F/R, pLJJ161-2-F/R, pLJJ161-3-F/R, pLJJ39-3-F/R, pLJJ161-4-F/R, pLJJ161-5-F/R, and pLJJ162-2-F/R, respectively.

For the construction of pLJJ164, the sgRNA of *ypl062w* were amplified with the primers pLJJ164-1-F/pLJJ149-1-R using sgRNA as a template. The truncated *URA3* was amplified from plasmid KIURA3 with primers pLJJ151-2-F/R. The above fragments were cloned into the *BsaI* site of pCAS.

pLJJ123 was constructed to overexpress *PEX11*. For the construction of pLJJ123, the LB of 805a, promoter of *GAL2*, *PEX11*, terminator of *PGK1*, *TRP1*, and RB of 805a were amplified with the primers pLJJ123-1-F/R, pLJJ123-2-F/R, pLJJ123-3-F/R, pLJJ161-5-F/R, pLJJ123-4-F/R, and pLJJ123-5-F/R, respectively.

pLJJ125 and pLJJ126 was constructed to overexpress *vps1*. For the construction of pLJJ125, the LB of 511b, promoter of *GAL10*, *VPS1*, terminator of *PGK1*, and RB of 511b were amplified with the primers pLJJ125-1-F/R, pLJJ125-2-F/R, pLJJ125-3-F/R, pLJJ161-5-F/R, and pLJJ125-4-F/R, respectively. For the construction of pLJJ126, the sgRNA of 511b were amplified with the primers pLJJ126-1-F/pLJJ149-1-R using sgRNA as a template. The truncated *URA3* was amplified from plasmid KIURA3 with primers pLJJ151-2-F/R. The above fragments were cloned into the *BsaI* site of pCAS.

pLJJ117, pLJJ118, pLJJ119, and pLJJ120 was constructed to delete *PEX30*, *PEX31*, and *PEX32*. For the construction of pLJJ117, the LB of *PEX30*, and RB of *PEX30* were amplified with the primers pLJJ117-1-F/R and pLJJ117-2-F/R. For the construction of pLJJ118, the LB of *PEX31* and RB of *PEX31* were amplified with the primers pLJJ118-1-F/R and pLJJ118-2-F/R. For the construction of pLJJ119, the LB of *PEX32*, and RB of *PEX32* were amplified with the primers pLJJ119-1-F/R and pLJJ119-2-F/R. For the construction of pLJJ120, the sgRNA of *PEX30*, the sgRNA of *PEX31*, and the sgRNA of *PEX32* were amplified with the primers pLJJ120-1-F/R, pLJJ120-2-F/R, and pLJJ120-4-F/R using sgRNA as a template. The truncated *URA3* was amplified from plasmid KIURA3 with primers pLJJ120-3-F/R. The above fragments were cloned into the *BsaI* site of pCAS.

pLJJ190 and pLJJ191 were constructed to delete *ACO1*. For the construction of pLJJ190, the LB of *ACO1* and RB of *ACO1* were amplified with the primers pLJJ190-1-F/R and pLJJ190-2-F/R. For the construction of pLJJ191, the sgRNA of *ACO1* was amplified with the primers pLJJ191-1-F/pLJJ149-1-R using sgRNA as a template. The truncated *URA3* was amplified from plasmid KIURA3 with primers pLJJ151-2-F/R. The above fragments were cloned into the *BsaI* site of pCAS.

pLJJ189 was constructed to delete *ADH1*. For the construction of pLJJ189, the LB of *ADH1*, *TRP1*, and RB of *ADH1* were amplified with the primers pLJJ189-1-F/R, pLJJ189-2-F/R, and pLJJ189-3-F/R, respectively.

pLJJ192 and pLJJ193 was constructed delete *MLS1*. For the construction of pLJJ192, the LB of *MLS1* and RB of *MLS1* were amplified with the primers pLJJ192-1-F/R and pLJJ192-2-F/R, respectively. For the construction of pLJJ193, the sgRNA of *MLS1* was amplified with the primers pLJJ193-1-F/pLJJ149-1-R using sgRNA as a template. The truncated *URA3* was amplified from plasmid KIURA3 with primers pLJJ151-2-F/R. The above fragments were cloned into the *BsaI* site of pCAS.

pLJJ194 and pLJJ195 was constructed to delete *CIT2*. For the construction of pLJJ194, the LB of *CIT2* and RB of *CIT2* were amplified with the primers pLJJ194-1-F/R and pLJJ194-2-F/R, respectively. For the construction of pLJJ195, the sgRNA of *CIT2* was amplified with the primers pLJJ195-1-F/pLJJ149-1-R using sgRNA as a template. The truncated *URA3* was amplified from plasmid KIURA3 with primers pLJJ151-2-F/R. The above fragments were cloned into the *BsaI* site of pCAS.

pLJJ198 and pLJJ199 was constructed to express *ALD2* and *ALD6*. For the construction of pLJJ198, the LB of 1309a, terminator of *CYC1*, *ALD2*, promoter of *GAL10* and *GAL1*, *ALD6*, terminator of *PGK1*, and RB of 1309a were amplified with the primers pLJJ198-1-F/R, pLJJ39-1-F/R, pLJJ198-2-F/R, pLJJ39-3-F/R, pLJJ198-3-F/R, pLJJ42-3-F/R, and pLJJ198-4-F/R, respectively. For the construction of pLJJ199, the sgRNA of 1309a was amplified with the primers pLJJ199-1-F/pLJJ149-1-R using sgRNA as a template. The truncated *URA3* was amplified from plasmid KIURA3 with primers pLJJ151-2-F/R. The above fragments were cloned into the *BsaI* site of pCAS.

pLJJ200 and pLJJ201 was constructed to express *ACS1* and *ACS2*. For the construction of pLJJ200, the LB of 1414a, terminator of *CYC1*, *ACS1*, promoter of *GAL10* and *GAL1*, *ACS2*, terminator of *PGK1*, and RB of 1414a were amplified with the primers pLJJ200-1-F/R, pLJJ39-1-F/R, pLJJ200-2-F/R, pLJJ39-3-F/R, pLJJ200-3-F/R, pLJJ42-3-F/R, and pLJJ200-4-F/R, respectively. For the construction of pLJJ201, the sgRNA of 1414a was amplified with the primers pLJJ201-1-F/pLJJ149-1-R using sgRNA as a template. The truncated *URA3* was amplified from plasmid KIURA3 with primers pLJJ151-2-F/R. The above fragments were cloned into the *BsaI* site of pCAS.

pLJJ196 and pLJJ197 was constructed to express *YIACL1*, *YIACL2*, and *CTP1*. For the construction of pLJJ196, the LB of 1014a, terminator of *CYC1*, *YIACL1*, promoter of *GAL10* and *GAL1*, *YIACL2*, terminator of *GAL10* and promoter of *GAL7*, *CTP1*, terminator of *ADH1*, and RB of 1014a were amplified with the primers pLJJ196-1-F/R, pLJJ39-1-F/R, pLJJ196-2-F/R, pLJJ39-3-F/R, pLJJ196-3-F/R, pLJJ39-5-F/R, pLJJ196-4-F/R, pLJJ39-7-F/R, and pLJJ196-5-F/R, respectively. For the construction of pLJJ197, the sgRNA of 1014a was amplified with the primers pLJJ197-1-F/pLJJ149-1-R using sgRNA as a template. The truncated *URA3* was amplified from plasmid KIURA3 with primers pLJJ151-2-F/R. The above fragments were cloned into the *BsaI* site of pCAS.

pLJJ132 and pLJJ134 were constructed to express *URA3*, *HIS3*, *LEU2*, and *TRP1*. For the construction of pLJJ132, the LB of *GAL80*, *URA3*, *HIS3*, *LEU2*, *TRP1*, and RB of *GAL80* were amplified with the primers pLJJ132-1-F/R, pLJJ132-2-F/R, pLJJ132-3-F/R, pLJJ132-4-F/R, pLJJ132-5-F/R, and pLJJ132-6-F/R, respectively. For the construction of pLJJ134, the sgRNA of *GAL80* was amplified with the primers pLJJ134-1-F/pLJJ149-1-R using sgRNA as a template. The truncated *URA3* was amplified from plasmid KIURA3 with primers pLJJ151-2-F/R. The above fragments were cloned into the *BsaI* site of pCAS.

#### 2.4. Shake-Flask Fermentation

Shake-flask fermentation was conducted as describe before [20]. The monoclonal of recombinant strains was inoculated into 3 mL YPD medium and cultured at 30 °C for 16–18 h. Then, 0.5 mL of the cultures was transferred into 50 mL YPDG medium and cultured at 30 °C for 3 days. Decane (10%) was used for in situ extraction and added into the cultures when the OD<sub>600</sub> reached approximately 0.8–1.

#### 2.5. Fed-Batch Fermentation for $\gamma$ -Bisabolene Biosynthesis

Fed-batch fermentation was conducted in a 5-L bioreactor (Shanghai Baoxing Biological Equipment Engineering Co., Ltd., Shanghai, China). Complete synthetic medium CSM (per liter, KH<sub>2</sub>PO<sub>4</sub> 8 g, MgSO<sub>4</sub>·7H<sub>2</sub>O 6.15 g, (NH<sub>4</sub>)<sub>2</sub>SO<sub>4</sub> 15 g, and glucose 40 g) was used [20]. The chemical compositions of the vitamin solution and trace metal solution were as described before. These solutions were added to CSM at concentrations of 10 mL/L and 12 mL/L when needed [20]. Feeding solution I consisted of 500 g/L glucose, 5.12 g/L MgSO<sub>4</sub>, 9 g/L KH<sub>2</sub>PO<sub>4</sub>, 0.28 g/L, Na<sub>2</sub>SO<sub>4</sub>, and 3.5 g/L K<sub>2</sub>SO<sub>4</sub>. The monoclonal of the engineered strain was cultured in 3 mL YPD medium for 16–18 h at 30 °C and 220 rpm. Subsequently, 1% of the culture was added to 200 mL YPD medium for another 16–18 h of cultivation at 30 °C as the seed culture. Then, the seed culture was transferred into 2 L CSM medium for fed-batch fermentation. A two-stage fermentation strategy was used. Feeding solution I was used for rapid cell growth in the first fermentation stage. When the residual glucose was below 1 g/L, the feeding solution was added into fermentation cultures to maintain the glucose concentration at around 1 g/L. Ethanol was used as feeding solution II. The temperature was maintained at 30 °C. The dissolved oxygen was maintained at 10–30%. The pH was controlled at 5.0 with the automatic addition of NH<sub>3</sub>·H<sub>2</sub>O. Glucose and ethanol were detected using a bioanalyzer (SBA-40C, Shandong Academy of Sciences, Jinan, China). The fermentation was terminated when the product production stopped increasing.

#### 2.6. Analytical Methods

After shake-flask fermentation, the fermentation cultures were centrifuged at 8000 rpm for 10 min. Then, the decane phase was collected and filtered for analysis. GC-MS (Agilent Technologies 7890A gas chromatograph equipped with 5975C inert XL MSD, Agilent Technologies Inc., Palo Alto, CA, USA) was used for the quantification of  $\gamma$ -bisabolene. Initially, the oven temperature was held at 50 °C for 1 min; then, the oven temperature was increased at a rate of 50 °C/min to 100 °C and was then held for 1 min. Subsequently, the oven temperature was increased at a rate of 20 °C/min to 280 °C and held for 2 min. The product was analyzed in total ion monitoring mode.

### 3. Results and Discussion

#### 3.1. Functional Characterization and Sequence Analysis of AcTPS5

In a previous report, *Actps5* was cloned; however, the major product catalyzed by AcTPS5 (GenBank Accession No. KFH42720.1), which accounted for >96% of total products detected, was unknown [20]. To confirm the structure of the major product, strain LSc5 was fermented in YPDGH medium, and the products were analyzed by GC-MS. As shown in Figure 1, peak 1 exhibited a mass fragmentation pattern with a parent ion at 204 *m/z*, which is typical for a sesquiterpene. Peak 1 was further identified as  $\gamma$ -bisabolene based on the characteristic daughter ions at 93.1, 107.1, 119.1, and 134.1 *m/z*, which is consistent with the standard EI mass spectral library, as reported in the literature [21].

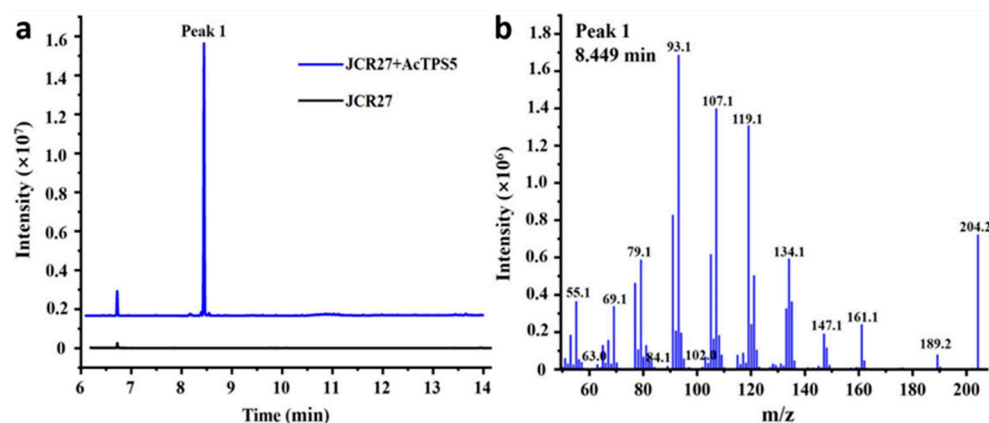


**Figure 1.** Analysis of volatile organic products from yeast transformants expressing AcTPS5 by GC-MS. (a) Total ion current chromatogram obtained from GC-MS analysis. Peak 1 corresponds to the major product. JCR27, JCR27 strain; JCR27 + AcTPS5, expressing AcTPS5 in JCR27 strain. (b) EI mass spectrum of the peak 1.

For sequence analysis of AcTPS5, 14 sequences of the reported bisabolene synthases were retrieved from a public database and references (Table S1). Sequence alignment revealed that AcTPS5 showed very low homology with bisabolene synthases from different species (Figure S14). The highest homology protein was PcSTS-08 (GenBank Accession No. BCX55502.1) from *Phanerochaete chrysosporium*, with a 30.80% identity. PcSTS-08 is known to be involved in the biosynthesis of (E)- $\alpha$ -bisabolene [22]. To gain insight into the evolutionary relationship between AcTPS5 and bisabolene synthases, a phylogenetic analysis was performed. The results showed that AcTPS5 and the bisabolene synthases were clustered into two subclades, where the bisabolene synthases derived from plants were clustered together, and bisabolene synthases Tps1A, Tps2A, PcSTS-08, and NvIDS1 were found to be evolutionarily related to AcTPS5. AcTPS5 was closely related to the (E)- $\alpha$ -bisabolene synthase PcSTS-08 identified from *P. chrysosporium* (Figure S15).

### 3.2. Producing $\gamma$ -Bisabolene in *S. cerevisiae* Peroxisomes

Considering the importance of  $\gamma$ -bisabolene and the high catalytic efficiency of AcTPS5, we intended to engineer *S. cerevisiae* for the efficient production of  $\gamma$ -bisabolene. In *S. cerevisiae*, peroxisomes play a crucial role as cell detoxification organelles; they may also provide an endogenous acetyl-CoA pool for terpene synthesis through fatty acid  $\beta$ -oxidation [15]. Previous studies have shown that the utilization of peroxisome FPP limits  $\alpha$ -humulene overproduction in peroxisomes [16]. In order to increase FPP supply in peroxisomes, as shown in Figure 2a, we overexpressed the MVA pathway genes with the enhanced peroxisome targeting signal (ePTS1) added to the C-terminal in JCR27, in which the additional copies of MVA pathway related genes, including *ERG10*, *ERG13*, *tHMG1*, *ERG12*, *ERG8*, *MVD1*, and *IDI*, were expressed in cytosol [23]. GAL promoters were used for high efficiency and rapid induction of sesquiterpene production once glucose was exhausted [20,24]. Modules M5, M6, M7, and M8 (Figures 2b and S5–S8) were created and integrated into the *GAL1* (encoding galactokinase [25]), 911b (ChrIX 127132-129160 [26]), *LPP1* (encoding lipid phosphate phosphatase), and *LEU2* (3-isopropylmalate dehydrogenase) gene loci, respectively, generating peroxisome chassis JCR29 (Figure 2b).

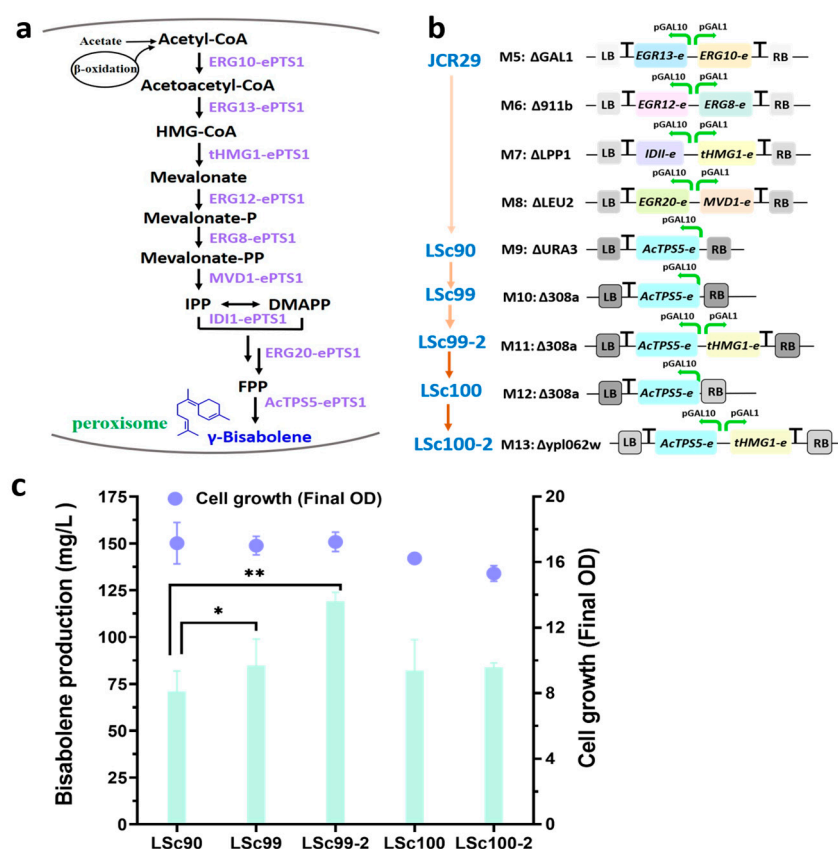


**Figure 2.** Bisabolene production with the constructed MVA pathway in peroxisomes (a). The MVA pathway constructed in peroxisomes. The expressed genes are depicted in purple. (b). The engineered strains integrated into different gene modules. These modules were integrated into the following chromosomal sites: *GAL1* (module 5, Chromosome II), 911b (module 6, Chromosome IX), *LPP1* (module 7, Chromosome IV), *LEU2* (module 8, Chromosome III), *URA3* (module 9, chromosome V), 308a (module 10, chromosome III), and *ypl1062w* (module 11, chromosome XVI). (c).  $\gamma$ -bisabolene production and cell growth in different engineered stains. The error bars represent standard deviations from three independent experiments. \*,  $p < 0.05$ ; \*\*,  $p < 0.01$ .

Next, the M9 (Figures 2b and S9) construct, consisting of *Actps5* fused with C-terminal ePTS1, was integrated into the *URA3* gene locus of JCR29, generating LSc90, which produced  $\gamma$ -bisabolene in peroxisomes. As shown in Figure 2c, bisabolene production in LSc90 reached a titer of 72.7 mg/L. The OD<sub>600</sub> of LSc90 showed an increase compared to the peroxisome chassis JCR29 (Figure 2c). Increasing *tHMG1* and the sesquiterpene synthase encoding gene copy numbers has been proven to be an efficient strategy to enhance target production in cytoplasm [20]. To further increase  $\gamma$ -bisabolene production in peroxisomes, another copy of *Actps5* was overexpressed through the M10 construct integrated into the 308a site (ChrIII 112601-114635 [26]) of LSc90, resulting in strain LSc99 (Figures 2b and S10). The  $\gamma$ -bisabolene production in LSc99 was 84.9 mg/L, and the biomass of LSc99 was consistent with LSc90 (Figure 2c), suggesting that the additional overexpression of one copy of *Actps5* in peroxisomes was beneficial for production generation. In addition, *Actps5*, together with *tHMG1*, was also overexpressed in LSc90 with the integration of the M11 construct into the 308a site (Figures 2b and S11); the resulting strain, LSc99-2, achieved a titer of 125.0 mg/L  $\gamma$ -bisabolene, displaying a 70% improvement compared to LSc90 (Figure 2c). This result indicates that increasing one copy of *Actps5* and *tHMG1* in peroxisomes is beneficial for  $\gamma$ -bisabolene generation.

Then, to further enhance  $\gamma$ -bisabolene production, another copy of *Actps5* was overexpressed. The M12 construct was integrated into the *ypl1062w* gene locus (ChrXVI 431895.4-32299 [27]) of LSc99-2, generating LSc100 (Figures 2b and S12). Meanwhile, the production

of  $\gamma$ -bisabolene was deduced in LSc100, and the biomass was also decreased, as shown in Figure 2c. In consideration of the effect of expressing *tHMG1*, another copy of *Actps5*, together with *tHMG1*, was also overexpressed in LSc99-2. The M13 construct was integrated into the *ypl062w* gene locus of LSc99-2, resulting in LSc100-2 (Figures 2b and S13). As a result,  $\gamma$ -bisabolene production and biomass of LSc100-2 were also deduced compared to the parent strain LSc99-2 (Figure 2c). The results indicate that in peroxisomes, excessive copies of *Actps5* are harmful for target generation, which might be because too much AcTPS5 protein in peroxisomes is toxic to yeast, and thus, the expression of AcTPS5 in peroxisomes should be tightly controlled.

### 3.3. Harnessing Peroxisomes to Enhance $\gamma$ -Bisabolene Production

The number of peroxisomes in *S. cerevisiae* is dependent on nutrient availability. The formation of new peroxisomes and the degradation of existing peroxisomes are tightly regulated in response to environmental signals [28]. The regulation of cytosolic peroxisome biogenesis is controlled by the *PEX* and *ATG* genes [28]. As shown in Figure 3a, *PEX11* was involved in peroxisome biogenesis fission in *S. cerevisiae*; the deletion of *pex11* results in enlarged peroxisomes, while the overexpression of *PEX11* increases the number of small peroxisomes [29]. Another gene, *VPS1*, is required for peroxisome division. A lack of *vps1* leads to a drastic decrease in peroxisomes [30]. Additionally, *PEX30*, *PEX31*, and *PEX32* are involved in the regulation of peroxisome size and number. The deletion of these three genes results in a significant increase of peroxisome numbers [30]. Peroxisome degradation was regulated by the deletion of the peroxisome autophagy gene, *atg36* [31].

Previous studies have shown that by modulating peroxisome populations, the production of geraniol was increased by 80% [32]. Therefore, we decided to regulate peroxisome numbers to increase bisabolene production in peroxisomes. The aforementioned six genes were knocked-out or overexpressed in various combinations in LSc99-2, resulting in 14 strains (LSc101–LSc114) (Figure 3b). Gene overexpression was achieved by replacing the native promoters with the *GAL1* promoter.

The engineered stains showed either a decline or an improvement in  $\gamma$ -bisabolene production compared to the parental strain, LSc99-2. Strains LSc103, LSc106, LSc108, LSc110, LSc112, LSc113, and LSc114, with the deletions of *pex30* $\Delta$ /*pex31* $\Delta$ /*pex32* $\Delta$ , exhibited an obvious decline of the cell growth, which might result in the decrease of bisabolene production (Figures 3b and S16). The results were consistent with the diminished growth of triple deletion *pex30* $\Delta$ /*pex31* $\Delta$ /*pex32* $\Delta$  yeast with monoterpene geraniol in the medium [17], indicating that *PEX30*, *PEX31*, and *PEX32* are crucial for yeast growth when terpenes are present. In addition, overexpressing *PEX11* or *VPS1* could improve bisabolene production, as shown in strains LSc101 (153.2 mg/L) and LSc102 (167.8 mg/L). The bisabolene titer was achieved at 164.7 mg/L in LSc105 overexpressing *PEX11* and *VPS1*. This result suggests that improving the peroxisome synthesis was effective for enhancing bisabolene production in yeast. Furthermore, the highest bisabolene production was observed in LSc104 with the deletion of *atg36*, with a 70% increase compared to the parent strain, reaching a titer of 216.9 mg/L (Figure 3b). Overexpressing *PEX11* or/and *VPS1*, together with deleting *atg36*, resulted in a decrease of bisabolene production compared to LSc104, as shown in LSc107 (162.9 mg/L), LSc109 (184.9 mg/L), and LSc111 (158.0 mg/L). The obtained results indicated that simultaneously regulating the synthesis and degradation of peroxisomes was adverse for product generation, and that the prevention of peroxisome degradation was more critical than the improvement in peroxisome synthesis for increasing  $\gamma$ -bisabolene production. Nevertheless, the production of  $\gamma$ -bisabolene was enhanced by modulating peroxisome populations.

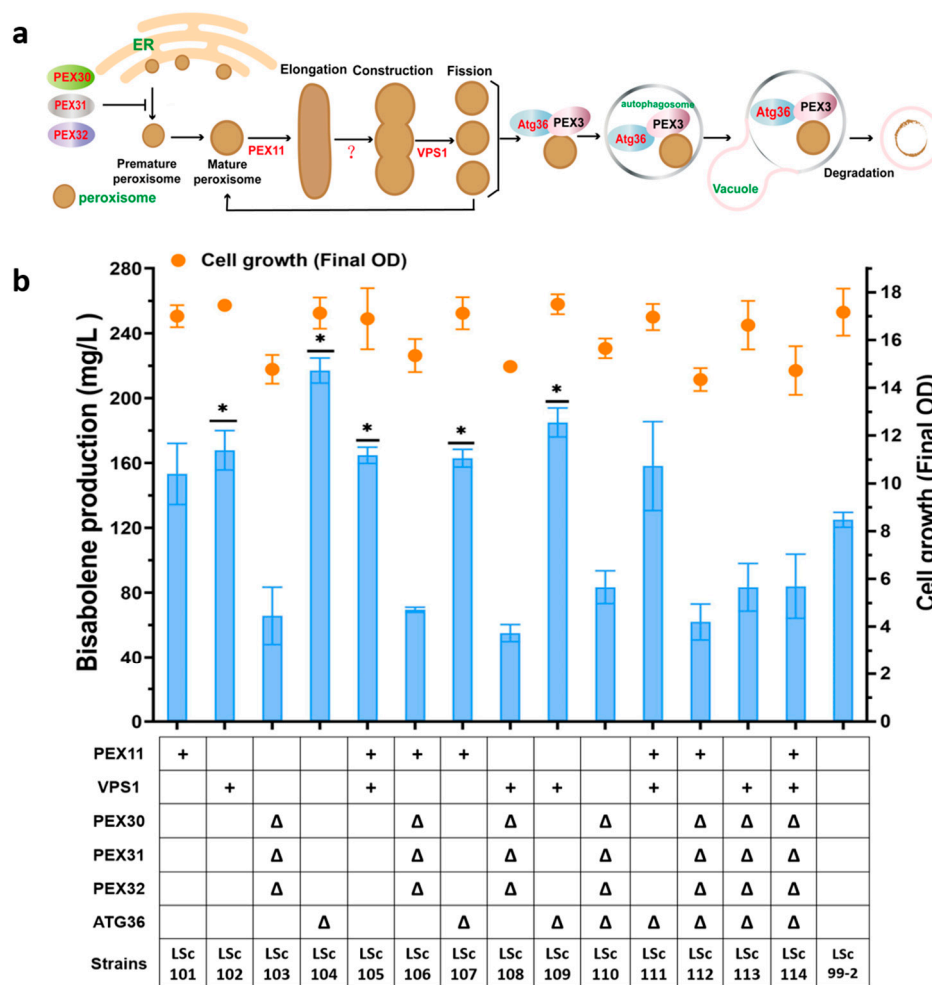


**Figure 3.** Engineering of peroxisomes to increase  $\gamma$ -bisabolene production. (a). A model of peroxisome biogenesis, division, and degradation. The modified genes are shown in red. ‘?’, the gene involved in this step is unclear. (b). Bisabolene production and cell growth in different engineered strains. +, overexpression of gene;  $\Delta$ , deletion of a gene. Error bars represent standard deviations from three independent experiments. \*,  $p < 0.05$ .

### 3.4. Dual Cytoplasmic-Peroxisomal Engineering to Optimize $\gamma$ -Bisabolene Production

It has been reported that taking advantage of the productivity of different compartments can dramatically enhance target production [33]. One approach for dual cytoplasmic-peroxisomal engineering is to introduce cytosolic expression genes into peroxisome strains to further improve  $\gamma$ -bisabolene production (Figure 4a). Multiple studies have shown that overexpressing the rate-limiting step enzymes, including tHMG1, ERG20, and the sesquiterpene synthetase, has a positive effect on the metabolic flux for sesquiterpene biosynthesis in yeast [32,34,35]. Therefore, a module (M1) was constructed for the cytoplasmic expression of *Actps5*, *ERG20*, and *tHMG1* (Figures 4b and S1). Five strains with higher peroxisome  $\gamma$ -bisabolene production, i.e., LSc102, LSc104, LSc105, LSc107, and LSc109, were chosen as the parent strains for cytoplasmic-peroxisomal engineering. The *ROX1* gene encodes a negative regulator of the MVA pathway, and the deletion of *Rox1* could increase the terpene production [36]. M1 was integrated into the *ROX1* gene locus of the five strains, resulting in LSc123, LSc115, LSc125, LSc128, and LSc130, respectively. The results showed that cell growth of these strains was not affected. LSc125, LSc128, and LSc130 exhibited obvious improvements in bisabolene production compared to their parent strains, with titers of 237.1 mg/L, 227.7 mg/L, 236.1 mg/L, respectively. The bisabolene production in LSc123 (163.5 mg/L) and LSc115 (205.8 mg/L) was close to that of the parent strains LSc102 (167.8 mg/L) and LSc104 (216.9 mg/L) (Figure 4b).

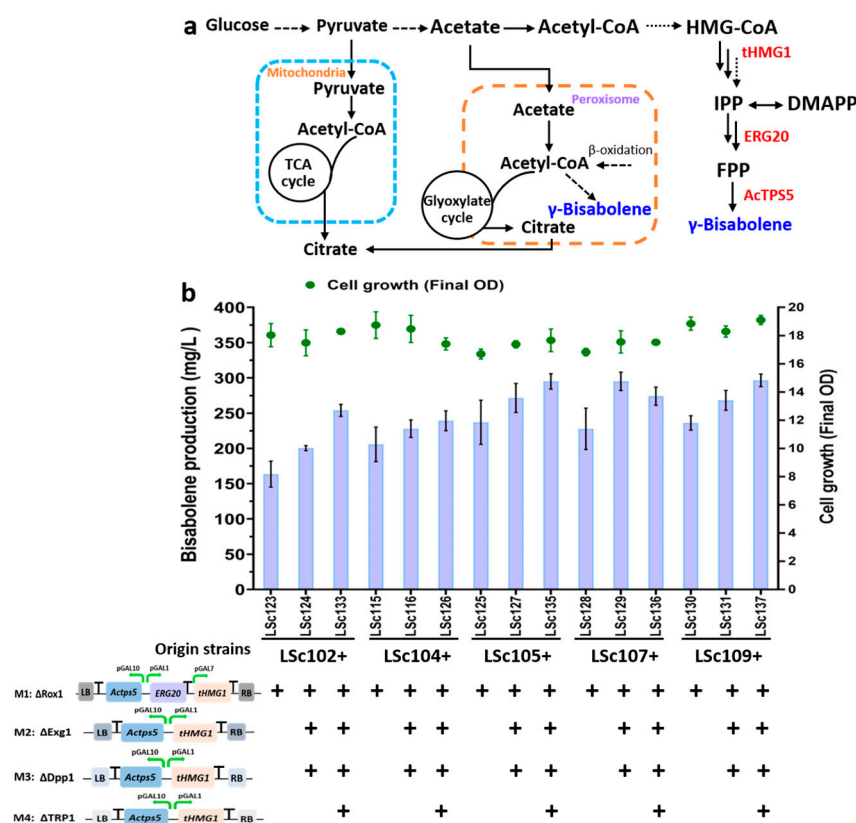


**Figure 4.** Dual cytoplasmic–peroxisomal engineering for bisabolene overproduction. (a). Schematic diagram of cytoplasmic–peroxisomal engineering. (b). Bisabolene production and cell growth in different engineered stains. The error bars represent the standard deviations from three independent experiments. These modules were integrated into the following chromosomal sites: *rox1* (module 1, Chromosome XIV), *exg1* (module 2, Chromosome XII), and *dpp1* (module 3, Chromosome IV), *trp1* (module 4, Chromosome IV). ‘+’, the module was introduced to the strain.

Increasing the gene copy numbers is an effective strategy to strengthen the target metabolic pathway flux in order to improve terpene production [37]. Therefore, another three modules with additional copy numbers of heterologously expressed genes were constructed, i.e., M2, M3, and M4 (Figures 4b and S2–S4). It was found that the loss of FPP could be decreased by deleting *DPP1*, which is beneficial for terpene production [38]. The growth rate of *exg1* deleting strain was similar to that of the wild-type strain [39]. *TRP1* is a yeast background defective gene, and its deletion would not affect strain growth. Hence, M2, M3, and M4 were introduced into the *EXG1*, *DPP1*, and *TRP1* gene loci of the LSc123, LSc115, LSc125, LSc128, and LSc130 strains. This resulted in the generation of ten engineered strains (Figure 4b). A noticeable increase in bisabolene production was observed compared to their respective parent strains. Three of the strains, namely, LSc135, LSc129, and LSc137 showed a 37% increase, with LSc137 reaching the highest titer of 296.4 mg/L of bisabolene. All ten engineered strains exhibited good cell growth, with an OD<sub>600</sub> greater than 17 (Figure 4b). These results indicated that dual cytoplasmic-peroxisomal engineering is beneficial for improving bisabolene production.

### 3.5. Engineering Acetyl-CoA Supply to Overproduce Bisabolene

Acetyl-CoA is a key metabolite that serves as a precursor for the production of various products, especially terpenoids. It has been reported that increasing the acetyl-CoA content can enhance the biosynthesis of downstream terpenes [40]. Therefore, we aimed to control acetyl-CoA supply to further improve bisabolene biosynthesis. Although cytoplasmic acetyl-CoA synthesis has been well studied [41], exploring the engineering of acetyl-CoA supply in cytoplasmic–peroxisomal producing strains to improve target production has

not been investigated to date. In this study, cytoplasmic–peroxisomal engineered strain LSc137 was used as the parent strain for subsequent experiments. As shown in Figure 5a, a strategy of increasing acetyl-CoA by overexpressing biosynthesis pathway genes and blocking other competing pathways genes was employed.

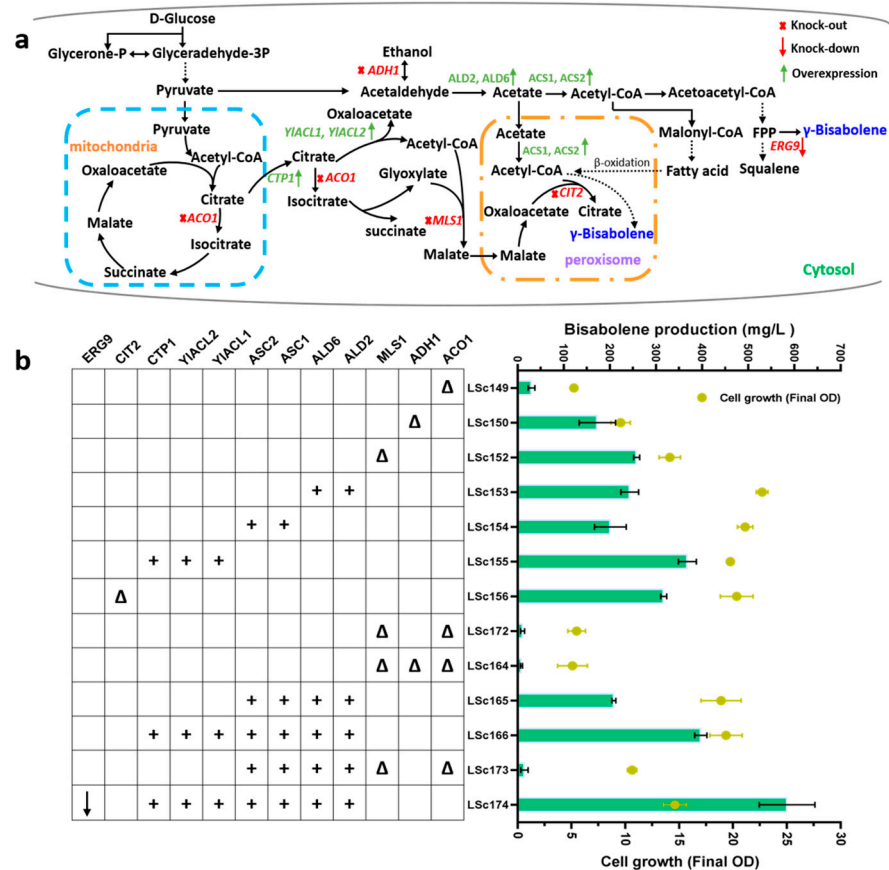


**Figure 5.** Bisabolene overproduction by engineering acetyl-CoA in *S. cerevisiae*. (a). Schematic diagram of acetyl-CoA engineering. Knocked-out and knock-down genes are marked in red. Over-expressed genes are marked in green. Red down arrow represents knock-down. (b). Bisabolene production and cell growth in different engineered stains.  $\Delta$ , knock-out; +, overexpression; down arrow, knock-down. Error bars represent the standard from three independent experiments.

Through overexpressing or deleting the genes involved in the metabolism of acetyl-CoA, twelve stains were obtained. In some of the resulting strains, the  $\gamma$ -bisabolene production was reduced. As shown in Figure 5b, with the deletion of *ACO1*, which encodes aconitase, a participant in the TCA cycle and glyoxylate cycle, severe growth defects and significant decreases in  $\gamma$ -bisabolene production were observed in LSc194, LSc172, LSc164, and LSc173 compared to the parent strain, LSc137 (296.4 mg/L, 19.1 OD<sub>600</sub>), suggesting that *ACO1* is essential for cytoplasmic–peroxisomal engineering strain survival and product generation. The deletion of alcohol dehydrogenase encoding gene *ADH1* or malate synthase encoding gene *MLS1* led to a decrease in the production of  $\gamma$ -bisabolene to 173 mg/L and 258.3 mg/L in strains LSc150 and LSc152, respectively, which was different to previous findings, i.e., that *MLS1* deletion could increase butanol production in a cytoplasmic engineering strain [42]. The results indicate that *MLS1* is important for cytoplasmic–peroxisomal bisabolene biosynthesis.

On the other hand, deletion of the peroxisomal citrate synthase encoding gene *CIT2* increased  $\gamma$ -bisabolene production to 317.0 mg/L in strain LSc156, indicating that increasing the peroxisomal acetyl-CoA was beneficial for product generation. Overexpressing transmembrane protein encoding gene *CTP1* and citrate lyases *YIACL1* and *YIACL2* from

*Yarrowia lipolytica* improved the  $\gamma$ -bisabolene titer to 368.1 mg/L in strain LSc155. However, overexpression of the aldehyde dehydrogenase encoding genes *ALD2* and *ALD6* and acetyl-CoA synthetase encoding genes *ACS1* and *ACS2* in the parent strain limited bisabolene production, as seen in strain LSc165 (208.9 mg/L) (Figure 5b). Overexpression of *ALD2*, *ALD6*, *ACS1*, and *ACS2* in LSc155 slightly enhanced the  $\gamma$ -bisabolene titer to 397.3 mg/L in LSc166; this might have been because the overexpression of *CTP1*, *YIACL1*, and *YIACL2* promoted acetyl-CoA metabolic flux, and the malate concentration was increased in peroxisome. Additionally, with the strengthening of *ACS1* and *ACS2*, more  $\gamma$ -bisabolene was synthesized in peroxisome, and thus,  $\gamma$ -bisabolene production was increased in LSc166.

The downregulation of *ERG9* (encoding squalene synthase) using the glucose-regulated  $P_{HXT1}$  promoter could increase  $\alpha$ -santalene production [43]. Therefore, to further improve the  $\gamma$ -bisabolene production in strain LSc166, the promoter of *ERG9* was replaced by the  $P_{HXT1}$  promoter and generated strain LSc174, achieving a titer of 584.14 (mg/L)  $\gamma$ -bisabolene with a modest decrease of cell growth (14.62 OD<sub>600</sub>) (Figure 5b). In summary, we successfully enhanced  $\gamma$ -bisabolene production by controlling the supply of acetyl-CoA in the cytoplasmic-peroxisomal strain.

### 3.6. High-Density Fermentation for $\gamma$ -Bisabolene Production

To obtain a prototrophic strain capable of surviving in synthetic basic medium CSM, LSc174 was transformed with *URA3*, *TRP1*, *LEU2*, and *HIS3*, generating strain LSc175 for fed-batch fermentation in a 5-L bioreactor. The results of fed-batch fermentation are shown in Figure 6. The residual glucose concentration reached 0.1 g/L at 10.47 h. Feeding solution I was then added at an appropriate flow rate for cell growth. The cell biomass of LSc175 continued to increase, reaching an OD<sub>600</sub> of 130 at 34.77 h, and began to fluctuate and decrease. Ethanol concentration started to decrease at 24.46 h, and the feeding solution I was stopped to consume the excess ethanol. At 32.62 h, the ethanol concentration reached 7.1 g/L. Then, ethanol was added as feeding solution II to promote product accumulation. Ethanol was maintained at an appropriate level until the end of fermentation. The fermentation of the 5-L bioreactor lasted for 61.38 h, and the production of  $\gamma$ -bisabolene reached 2.69 g/L.

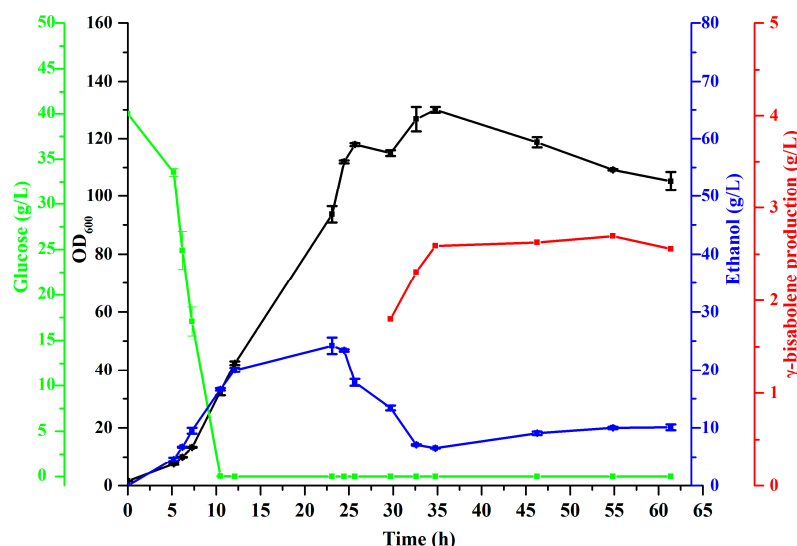


**Figure 6.** High-density fermentation of strain LSc175 for  $\gamma$ -bisabolene production. Results of fermentation in a 5-L bioreactor.  $\gamma$ -bisabolene production, cell growth, and residual amounts of glucose were measured. The error bars indicate the standard deviations of three replicates.

Although the  $\gamma$ -bisabolene production reached a high level with LSc175, the potential of the cytoplasm-peroxisome engineered strain was not fully realized during fed-batch fermentation, as reported [18].  $\gamma$ -bisabolene production reached 2.59 g/L at 34.7 h; however,

after that, the production of  $\gamma$ -bisabolene barely increased until the end of fermentation. We noticed that the engineered strain grew normally with glucose as the carbon source, while with ethanol as a carbon source, the growth of the strain showed an obvious decline. It was found that the disturbance of the peroxisome system leads to defects in the utilization of the corresponding carbon source [29,44]. In strain LSc175, the autophagic degradation of peroxisomes was inhibited with the deletion of *atg36*, meaning that the maintenance of the highly dynamic peroxisomal system was abolished, which might give rise deficient cell growth with ethanol as a carbon source and counterproductively affect the synthesis of  $\gamma$ -bisabolene. Thus, regulating the glucose feeding rate to downregulate ethanol accumulation during the first stage of fed-batch fermentation and replacing ethanol with another carbon source, such as sucrose, as the second phase feeding solution [45] may improve the productivity with fed-batch fermentation. Nevertheless, the cytoplasm–peroxisome engineered strain exhibited great potential for overproducing  $\gamma$ -bisabolene.

#### 4. Conclusions

In this study, we successfully achieved high production of  $\gamma$ -bisabolene through dual cytoplasmic–peroxisomal engineering in *S. cerevisiae*. A novel  $\gamma$ -bisabolene synthase was identified and applied for  $\gamma$ -bisabolene biosynthesis. By expressing  $\gamma$ -bisabolene both in cytosol and peroxisomes, as well as enhancing the availability of the precursor, i.e., acetyl-CoA, we were able to achieve the highest reported titer of  $\gamma$ -bisabolene at 2.69 g/L in a 5 L fed-batch fermentation. This study demonstrates a promising approach for the efficient production of sesquiterpenes.

**Supplementary Materials:** The following supporting information can be downloaded at: <https://www.mdpi.com/article/10.3390/fermentation9090779/s1>. Table S1: bisabolene synthases from different organisms. Table S2: Strains and plasmids. Table S3: Primers. Figure S1: Plasmid map for expressing M1 module. Figure S2: Plasmid map for expressing M2 module. Figure S3: Plasmid map for expressing M3 module. Figure S4: Plasmid map for expressing M4 module. Figure S5: Plasmid map for expressing M5 module. Figure S6: Plasmid map for expressing M6 module. Figure S7: Plasmid map for expressing M7 module. Figure S8: Plasmid map for expressing M8 module. Figure S9: Plasmid map for expressing M9 module. Figure S10: Plasmid map for expressing M10 module. Figure S11: Plasmid map for expressing M11 module. Figure S12: Plasmid map for expressing M12 module. Figure S13: Plasmid map for expressing M13 module. Figure S14: Amino acids alignment of AcPS5 reported bisabolene synthases. Figure S15: Phylogenetic analysis of AcTPS5 and bisabolene synthases from other species. Figure S16: Time course profiles of cell growth. References [46–56] are cited in the supplementary materials.

**Author Contributions:** J.L. carried out all the construction of strains and plasmids used in this study. J.L. drafted the manuscript. G.Y., X.W., F.W., P.H., S.B., K.W. and T.S. assisted with the experiment and analysis. H.J. revised the manuscript. All authors have read and agreed to the published version of the manuscript.

**Funding:** This research was funded by the State Key Laboratory of NBC Protection for Civilian (SKLNBC2022-07) of China.

**Institutional Review Board Statement:** Not applicable.

**Informed Consent Statement:** Not applicable.

**Data Availability Statement:** Data is contained within the article and Supplementary Material.

**Acknowledgments:** We are grateful to Tiangang Liu (School of Pharmaceutical Sciences, Wuhan University) for technical Assistance.

**Conflicts of Interest:** The authors declare no conflict of interest.

## References

1. Liu, C.L.; Xue, K.; Yang, Y.K.; Liu, X.X.; Li, Y.; Lee, T.; Bai, Z.; Tan, T. Metabolic engineering strategies for sesquiterpene production in microorganism. *Crit. Rev. Biotechnol.* **2022**, *42*, 3–92. [[CrossRef](#)] [[PubMed](#)]
2. Jiang, H.; Wang, X. Biosynthesis of monoterpenoid and sesquiterpenoid as natural flavors and fragrances. *Biotechnol. Adv.* **2023**, *65*, 108151. [[CrossRef](#)] [[PubMed](#)]
3. Hewage, R.T.; Tseng, C.C.; Liang, S.; Lai, C.Y.; Lin, H.C. Genome mining of cryptic bisabolenes that were biosynthesized by intramembrane terpene synthases from *Antrodia cinnamomea*. *Philos. Trans. R. Soc. Lond. B Biol. Sci.* **2023**, *378*, 20220033. [[CrossRef](#)] [[PubMed](#)]
4. Peralta-Yahya, P.P.; Ouellet, M.; Chan, R.; Mukhopadhyay, A.; Keasling, J.D.; Lee, T.S. Identification and microbial production of a terpene-based advanced biofuel. *Nat. Commun.* **2011**, *2*, 483. [[CrossRef](#)]
5. Kamatou, G.P.P.; Viljoen, A.M. A review of the application and pharmacological properties of alpha-bisabolol and alpha-bisabolol-rich oils. *J. Am. Oil Chem. Soc.* **2010**, *87*, 1–7. [[CrossRef](#)]
6. Yeo, S.K.; Ali, A.Y.; Hayward, O.A.; Turnham, D.; Jackson, T.; Bowen, I.D.; Clarkson, R.  $\beta$ -Bisabolene, a sesquiterpene from the essential oil extract of *Opoponax* (*Commiphora guidottii*), exhibits cytotoxicity in breast cancer cell lines. *Phytother. Res.* **2016**, *30*, 418–425. [[CrossRef](#)]
7. Nascimento, A.M.; Brandao, M.G.; Oliveira, G.B.; Fortes, I.C.; Chartone-Souza, E. Synergistic bactericidal activity of *Eremanthus erythropappus* oil or  $\beta$ -bisabolene with ampicillin against *Staphylococcus aureus*. *Antonie Leeuwenhoek.* **2007**, *92*, 95–100. [[CrossRef](#)]
8. Shu, H.Z.; Peng, C.; Bu, L.; Guo, L.; Liu, F.; Xiong, L. Bisabolane-type sesquiterpenoids: Structural diversity and biological activity. *Phytochemistry* **2021**, *192*, 112927. [[CrossRef](#)]
9. Jou, Y.J.; Hua, C.H.; Lin, C.S.; Wang, C.Y.; Wan, L.; Lin, Y.J.; Huang, S.H.; Lin, C.W. Anticancer activity of  $\gamma$ -bisabolene in human neuroblastoma cells via induction of p53-mediated mitochondrial apoptosis. *Molecules* **2016**, *21*, 601. [[CrossRef](#)]
10. Govindarajan, M.; Vaseeharan, B.; Alharbi, N.S.; Kadaikunnan, S.; Khaled, J.M.; Al-Anbr, M.N.; Alyahya, S.A.; Maggi, F.; Benelli, G. High efficacy of (Z)- $\gamma$ -bisabolene from the essential oil of *Galinsoga parviflora* (Asteraceae) as larvicide and oviposition deterrent against six mosquito vectors. *Environ. Sci. Pollut. Res. Int.* **2018**, *25*, 10555–10566. [[CrossRef](#)]
11. Lim, D.S.; Shi, L.L.; Guo, K.; Luo, S.; Liu, Y.; Chen, Y.; Liu, Y.; Li, S.H. A new sesquiterpene synthase catalyzing the formation of (R)- $\beta$ -bisabolene from medicinal plant *Colquhounia coccinea* var. *mollis* and its anti-adipogenic and antibacterial activities. *Phytochemistry* **2023**, *211*, 113681.
12. Chemat, F.; Vian, M.A.; Cravotto, G. Green extraction of natural products: Concept and principles. *Int. J. Mol. Sci.* **2012**, *13*, 8615–8627. [[CrossRef](#)] [[PubMed](#)]
13. Walls, L.E.; Otoupal, P.; Ledesma-Amaro, R.; Velasquez-Orta, S.B.; Gladden, J.M.; Rios-Solis, L. Bioconversion of cellulose into bisabolene using *Ruminococcus flavefaciens* and *Rhodospiridium toruloides*. *Bioresour. Technol.* **2023**, *368*, 128216. [[CrossRef](#)] [[PubMed](#)]
14. Zhao, Y.; Zhu, K.; Li, J.; Zhao, Y.; Li, S.L.; Zhang, C.; Xiao, D.; Yu, A.Q. High-efficiency production of bisabolene from waste cooking oil by metabolically engineered *Yarrowia lipolytica*. *Microb. Biotechnol.* **2021**, *14*, 2497–2513. [[CrossRef](#)] [[PubMed](#)]
15. Kulagina, N.N.; Besseau, S.; Papon, N.; Courdavault, V. Peroxisomes: A New Hub for Metabolic Engineering in Yeast. *Front. Bioeng. Biotechnol.* **2021**, *9*, 659431. [[CrossRef](#)] [[PubMed](#)]
16. Zhang, C.B.; Li, M.; Zhao, G.; Lu, W.Y. Harnessing Yeast Peroxisomes and cytosol acetyl-CoA for sesquiterpene  $\alpha$ -Humulene production. *J. Agric. Food Chem.* **2020**, *68*, 1382–1389. [[CrossRef](#)]
17. Gerke, J.; Frauendorf, H.; Schneider, D.; Wintergoller, M.; Hofmeister, T.; Poehlein, A.; Zebec, Z.; Takano, E.; Scrutton, N.S.; Braus, G.H. Production of the fragrance geraniol in peroxisomes of a product-tolerant baker's yeast. *Front. Bioeng. Biotechnol.* **2020**, *8*, 582052. [[CrossRef](#)]
18. Liu, G.S.; Li, T.; Zhou, W.; Jiang, M.; Tao, X.Y.; Liu, M.; Zhao, M.; Ren, Y.; Gao, B.; Wang, F.Q.; et al. The yeast peroxisome: A dynamic storage depot and subcellular factory for squalene overproduction. *Metab. Eng.* **2020**, *57*, 151–161. [[CrossRef](#)]
19. Hammer, S.K.; Avalos, J.L. Harnessing yeast organelles for metabolic engineering. *Nat. Chem. Biol.* **2017**, *13*, 823–832. [[CrossRef](#)]
20. Liu, J.J.; Chen, C.; Wan, X.K.; Yao, G.; Bao, S.H.; Wang, F.L.; Wang, K.; Song, T.Y.; Han, P.G.; Jiang, H. Identification of the sesquiterpene synthase AcTPS1 and high production of (–)-germacrene D in metabolically engineered *Saccharomyces cerevisiae*. *Microb. Cell Fact.* **2022**, *21*, 89. [[CrossRef](#)]
21. Rinkel, J.; Dickschat, J.S. Stereochemical investigations on the biosynthesis of achiral (Z)- $\gamma$ -bisabolene in *Cryptosporangium arvom.* *Beilstein J. Org. Chem.* **2019**, *15*, 789–794. [[CrossRef](#)] [[PubMed](#)]
22. Ichinose, H.; Ukeba, S.; Kitaoka, T. Latent potentials of the white-rot basidiomycete *Phanerochaete chrysosporium* responsible for sesquiterpene metabolism: CYP5158A1 and CYP5144C8 decorate (E)- $\alpha$ -bisabolene. *Enzym. Microb. Technol.* **2022**, *158*, 110037. [[CrossRef](#)] [[PubMed](#)]
23. Siemon, T.; Wang, Z.Q.; Bian, G.K.; Seitz, T.; Ye, Z.L.; Lu, Y.; Cheng, S.; Ding, Y.K.; Huang, Y.L.; Deng, Z.X.; et al. Semisynthesis of plant-derived englerin A enabled by microbe engineering of guaia-6,10(14)-diene as building block. *J. Am. Chem. Soc.* **2020**, *142*, 2760–2765. [[CrossRef](#)]
24. Wang, F.; Lv, X.; Xie, W.; Zhou, P.; Zhu, Y.; Yao, Z.; Yang, C.; Yang, X.; Ye, L.; Yu, H. Combining Gal4p-mediated expression enhancement and directed evolution of isoprene synthase to improve isoprene production in *Saccharomyces cerevisiae*. *Metab. Eng.* **2017**, *39*, 257–266. [[CrossRef](#)] [[PubMed](#)]

25. Jiang, G.Z.; Yao, M.D.; Wang, Y.; Zhou, L.; Song, T.; Liu, H.; Xiao, W.H.; Yuan, Y.J. Manipulation of GES and ERG20 for geraniol overproduction in *Saccharomyces cerevisiae*. *Metab. Eng.* **2017**, *41*, 57–66. [[CrossRef](#)] [[PubMed](#)]
26. Apel, A.R.; d'Espaux, L.; Wehrs, M.; Sachs, D.; Li, R.A.; Tong, G.J.; Garber, M.; Nnadi, O.; Zhuang, W.; Hillson, N.; et al. A Cas9-based toolkit to program gene expression in *Saccharomyces cerevisiae*. *Nucleic Acids Res.* **2017**, *45*, 496–508.
27. Chen, Y.; Wang, Y.; Liu, M.; Qu, J.Z.; Yao, M.D.; Li, B.; Ding, M.Z.; Liu, H.; Xiao, W.H.; Yuan, Y.J. Primary and secondary metabolic effects of a key gene deletion ( $\Delta ypl062w$ ) in metabolically engineered terpenoid-producing *Saccharomyces cerevisiae*. *Appl. Environ. Microbiol.* **2019**, *85*, e01990-18. [[CrossRef](#)] [[PubMed](#)]
28. Akşit, A.; Klei, I.J. Yeast peroxisomes: How are they formed and how do they grow? *Int. J. Biochem. Cell Biol.* **2018**, *105*, 24–34. [[CrossRef](#)] [[PubMed](#)]
29. Rottensteiner, H.; Stein, K.; Sonnenhol, E.; Erdmann, R. Conserved Function of *Pex11p* and the Novel *Pex25p* and *Pex27p* in Peroxisome Biogenesis. *Mol. Biol. Cell* **2003**, *14*, 4316–4328. [[CrossRef](#)]
30. Fagarasanu, A.; Fagarasanu, M.; Rachubinski, R.A. Maintaining peroxisome populations: A story of division and inheritance. *Annu. Rev. Cell Dev. Biol.* **2007**, *23*, 321–344. [[CrossRef](#)]
31. Motley, A.M.; Nuttall, J.M.; Hetteema, E.H. Pex3-anchored Atg36 tags peroxisomes for degradation in *Saccharomyces cerevisiae*. *EMBO J.* **2012**, *31*, 2852–2868. [[CrossRef](#)]
32. Donald, K.A.G.; Hampton, R.Y.; Fritz, I.B. Effects of overproduction of the catalytic domain of 3-hydroxy-3-methylglutaryl coenzyme A reductase on squalene synthesis in *Saccharomyces cerevisiae*. *Appl. Environ. Microbiol.* **1997**, *63*, 3341–3344. [[CrossRef](#)]
33. Lv, X.M.; Wang, F.; Zhou, P.P.; Ye, L.D.; Xie, W.P.; Xu, H.M.; Yu, H.W. Dual regulation of cytoplasmic and mitochondrial acetyl-CoA utilization for improved isoprene production in *Saccharomyces cerevisiae*. *Nat. Commun.* **2016**, *7*, 12851. [[CrossRef](#)]
34. Jiang, Y.K.; Xia, L.; Gao, S.; Li, N.; Yu, S.Q.; Zhou, J.W. Engineering *Saccharomyces cerevisiae* for enhanced (–)- $\alpha$ -bisabolol production. *Synth. Syst. Biotechnol.* **2023**, *8*, 187–195. [[CrossRef](#)] [[PubMed](#)]
35. Deng, X.M.; Shi, B.; Ye, Z.L.; Huang, M.; Chen, R.; Cai, Y.S.; Kuang, Z.L.; Sun, X.; Bian, G.K.; Deng, Z.X.; et al. Systematic identification of *Ocimum sanctum* sesquiterpenoid synthases and (–)-eremophilene overproduction in engineered yeast. *Metab. Eng.* **2022**, *69*, 122–133. [[CrossRef](#)] [[PubMed](#)]
36. Henry, K.W.; Nickels, J.T.; Edlind, T.D. *ROX1* and *ERG* regulation in *Saccharomyces cerevisiae*: Implications for antifungal susceptibility. *Eukaryot. Cell* **2002**, *1*, 1041–1044. [[CrossRef](#)] [[PubMed](#)]
37. Xie, W.; Lv, X.; Ye, L.; Zhou, P.; Yu, H. Construction of lycopene-overproducing *Saccharomyces cerevisiae* by combining directed evolution and metabolic engineering. *Metab. Eng.* **2015**, *30*, 69–78. [[CrossRef](#)]
38. Faulkner, A.; Chen, X.; Rush, J.; Horazdovsky, B.; Waechter, C.J.; Carman, G.M.; Sternweis, P.C. The *LPP1* and *DPP1* gene products account for most of the isoprenoid phosphate phosphatase activities in *Saccharomyces cerevisiae*. *J. Biol. Chem.* **1999**, *274*, 14831–14837. [[CrossRef](#)]
39. Wang, H.M.; Yang, Y.; Lin, L.; Zhou, W.L.; Liu, M.Z.; Cheng, K.D.; Wang, W. Engineering *Saccharomyces cerevisiae* with the deletion of endogenous glucosidases for the production of flavonoid glucosides. *Microb. Cell Factories* **2016**, *15*, 134. [[CrossRef](#)]
40. Paramasivan, K.; Mutturi, S. Progress in terpene synthesis strategies through engineering of *Saccharomyces cerevisiae*. *Crit. Rev. Biotechnol.* **2017**, *37*, 974–989. [[CrossRef](#)]
41. Lian, J.Z.; Si, T.; Nair, N.U.; Zhao, H.M. Design and construction of acetyl-CoA overproducing *Saccharomyces cerevisiae* strains. *Metab. Eng.* **2014**, *24*, 139–149. [[CrossRef](#)] [[PubMed](#)]
42. Krivoruchko, A.; Amatriain, C.S.; Chen, Y.; Siewers, V.; Nielsen, J. Improving biobutanol production in engineered *Saccharomyces cerevisiae* by manipulation of acetyl-CoA metabolism. *J. Ind. Microbiol. Biotechnol.* **2013**, *40*, 1051–1056. [[CrossRef](#)] [[PubMed](#)]
43. Scalcinati, G.; Knuf, C.; Partow, S.; Chen, Y.; Maury, J.; Schalk, M.; Daviet, L.; Nielsen, J.; Siewers, V. Dynamic control of gene expression in *Saccharomyces cerevisiae* engineered for the production of plant sesquiterpene  $\alpha$ -santalene in a fed-batch mode. *Metab. Eng.* **2012**, *14*, 91–103. [[CrossRef](#)] [[PubMed](#)]
44. Idnurm, A.; Giles, S.S.; Perfect, J.R. Peroxisome function regulates growth on glucose in the basidiomycete fungus *Cryptococcus neoformans*. *Eukaryot. Cell* **2007**, *6*, 60–72. [[CrossRef](#)]
45. Vitolo, M.; Duranti, M.A.; Pellegrim, M.B. Effect of pH, aeration and sucrose feeding on the invertase activity of intact *S. cerevisiae* cells grown in sugarcane blackstrap molasses. *J. Ind. Microbiol.* **1995**, *15*, 75–79. [[CrossRef](#)] [[PubMed](#)]
46. Bohlmann, J.; Crock, J.; Jetter, R.; Croteau, R. Terpenoid-based defenses in conifers: cDNA cloning, characterization, and functional expression of wound-inducible (E)- $\alpha$ -bisabolene synthase from grand fir (*Abies grandis*). *Proc. Natl. Acad. Sci. USA* **1998**, *95*, 6756–6761. [[CrossRef](#)]
47. Huber, D.W.; Philippe, R.N.; Godard, K.A.; Sturrock, R.N.; Bohlmann, J. Characterization of four terpene synthase cDNAs from methyl jasmonate-induced Douglas-fir, *Pseudotsuga menziesii*. *Phytochemistry* **2005**, *66*, 1427–1439. [[CrossRef](#)]
48. Fujisawa, M.; Harada, H.; Kenmoku, H.; Mizutani, S.; Misawa, N. Cloning and characterization of a novel gene that encodes (S)-beta-bisabolene synthase from ginger, *Zingiber officinale*. *Planta* **2010**, *232*, 121–130. [[CrossRef](#)]
49. Parveen, I.; Wang, M.; Zhao, J.; Chittiboyina, A.G.; Tabanca, N.; Ali, A.; Baerson, S.R.; Techen, N.; Chappell, J.; Khan, I.A.; et al. Investigating sesquiterpene biosynthesis in *Ginkgo biloba*: Molecular cloning and functional characterization of (E,E)-farnesol and alpha-bisabolene synthases. *Plant Mol. Biol.* **2015**, *89*, 451–462. [[CrossRef](#)]
50. Srivastava, P.L.; Daramwar, P.P.; Krithika, R.; Pandreka, A.; Shankar, S.S.; Thulasiram, H.V. functional characterization of novel sesquiterpene synthases from indian sandalwood, *Santalum album*. *Sci. Rep.* **2015**, *5*, 10095. [[CrossRef](#)]

51. Ro, D.K.; Ehling, J.; Keeling, C.I.; Lin, R.; Mattheus, N.; Bohlmann, J. Microarray expression profiling and functional characterization of AtTPS genes\_ duplicated *Arabidopsis thaliana* sesquiterpene synthase genes. *Arch. Biochem. Biophys.* **2006**, *448*, 104–116. [[CrossRef](#)]
52. Aschenbrenner, A.K.; Kwon, M.; Conrad, J.; Ro, D.; Spring, O. Identification and characterization of two bisabolene synthases from linear glandular trichomes of sunflower (*Helianthus annuus* L., Asteraceae). *Phytochemistry* **2016**, *124*, 29–37. [[CrossRef](#)] [[PubMed](#)]
53. Lancaster, J.; Lehner, B.; Khimian, A.; Muchlinski, A.; Luck, K.; Köllner, T.G.; Weber, D.C.; Gundersen-Rindal, D.; Tholl, D. An IDS-Type sesquiterpene synthase produces the pheromone precursor (Z)- $\alpha$ -Bisabolene in *Nezara viridula*. *J. Chem. Ecol.* **2019**, *45*, 187–197. [[CrossRef](#)] [[PubMed](#)]
54. Zhang, X.; Niu, M.; Silva, J.T.; Zhang, Y.Y.; Yuan, Y.F.; Jia, Y.; Xiao, Y.; Li, Y.; Fang, L.; Zeng, S.; et al. Identification and functional characterization of three new terpene synthase genes involved in chemical defense and abiotic stresses in *Santalum album*. *BMC Plant Biol.* **2019**, *19*, 115. [[CrossRef](#)] [[PubMed](#)]
55. Muchlinski, A.; Chen, X.L.; Lovell, J.T.; Köllner, T.G.; Pelot, K.A.; Zerbe, P.; Ruggiero, M.; Callaway, L.; Laliberte, S.; Chen, F.; et al. Biosynthesis and emission of stress-induced volatile terpenes in roots and leaves of switchgrass (*Panicum virgatum* L.). *Front Plant Sci.* **2019**, *10*, 1144. [[CrossRef](#)] [[PubMed](#)]
56. Zhang, Y.P.; Wang, J.; Wang, Z.B.; Zhang, Y.M.; Shi, S.B.; Nielsen, J.; Liu, Z.H. A gRNA-tRNA array for CRISPR-Cas9 based rapid multiplexed genome editing in *Saccharomyces cerevisiae*. *Nat. Commun.* **2019**, *5*, 1053. [[CrossRef](#)]

**Disclaimer/Publisher’s Note:** The statements, opinions and data contained in all publications are solely those of the individual author(s) and contributor(s) and not of MDPI and/or the editor(s). MDPI and/or the editor(s) disclaim responsibility for any injury to people or property resulting from any ideas, methods, instructions or products referred to in the content.